The Influence of the Symbol Detection Error on Cooperative In-home Power Line Communication based on HS-OFDM Scheme

Michelle S. P. Facina[†] and Moises V. Ribeiro[†,*]
[†]UFJF - Federal University of Juiz de Fora, Brazil.
[*]Smarti9 Ltda. - Juiz de Fora, Brazil.

***Abstract*— This work analyzes the influence of symbol detection error on cooperative in-home power line communication based on channel estimates provided by a measurement campaign. We investigate cooperation communication based on a single relay model in which the relay node is situated in different locations between source and destination nodes by considering closed-form expressions of the maximum data rate of hermitian symmetric orthogonal frequency division multiplexing scheme with frequency domain equalizer based on minimum mean square error and zero-forcing criteria. The analysis is carried out over the amplify-and-forward (AF) and decode-and-forward (DF) protocols together with maximal ratio combining technique. Numerical results show that the advantage of the DF protocol relative to AF one ends when the symbol detection error achieves a threshold and this threshold depends upon relative location of the relay node regarding source and destination nodes.**

***Keywords*— Cooperative in-home PLC channel, maximum data rate, AF and DF protocols, symbol detection error.**

I. Introduction

A growing interest in the use of electric power grids for communication purposes is notorious. Indeed, power line communication (PLC) systems and their applications have been widely investigated by academic and business sectors. However, as electric power grids were not originally designed for communication purposes, they constitute a challenging data communication medium, in which the transmitted signals suffer severe attenuations and are strongly corrupted by colored and impulsive noise.

Currently, a promising alternative that has been studied to overcome these limitations is the use of cooperative communication concepts for PLC systems. Regarding to that, some investigations have been carried out to provide performance improvements, such as robustness, spectral efficiency and throughput. For example, [1] mentions that the spatial dimension of the PLC network becomes infeasible the direct communication between the central node and all other connected devices and, therefore, to achieve complete coverage, symbols need to be repeated, which is also known as multi hop transmission. This way, the data communication makes optimal use of the available communication nodes in the network and is flexible enough to also ensure coverage and communication reliability under different channel conditions. An opportunistic cooperative system to provide power saving, quality of service, coverage and range extension is discussed in [2]. In this context, the relay only acts in certain situations when the channel capacity related to the decode-and-forward (DF) protocol is higher than that achievable through the direct link.

Although these contributions investigate the suitability of cooperative concepts for improving PLC systems on in-home electric power grids, they do not analyze the influence of symbol detection error when the performance of the DF protocol is considered.

Aiming to fill this lack, in this paper, we compare the performance improvement that can be potentially offered by amplify-and-forward (AF) and DF protocols on in-home PLC systems, varying the symbol detection error at the relay. This is obtained with measured cooperative and in-home PLC channels when the frequency band is 1.7-100 MHz. By providing the best results according to [3], the maximal ratio combining (MRC) technique is deployed to combine the information transmitted by using a Hermitian-Symmetric Orthogonal Frequency Division Multiplexing (HS-OFDM) scheme [4]. The attained results reveal that there is a threshold of symbol detection error from that the DF protocol is not advantageous in relation to AF protocol.

Thereby, the following structure is followed: Section II presents the adopted assumptions. Section III describes the measurement campaign. Section IV presents numerical analyses of maximum data rates. Finally, concluding remarks are given in Section V.

II. Channel Analysis

The single relay model in which there are a source node (S), a relay node (R) and a destination node (D) is depicted in Fig. 1, where $\{h_{SD}[n]\}_{n=0}^{L_{h_{SD}}-1}$, $\{h_{SR}[n]\}_{n=0}^{L_{h_{SR}}-1}$, and $\{h_{RD}[n]\}_{n=0}^{L_{h_{RD}}-1}$ denote the discrete time representation of the linear and time-invariant impulse responses for the source-destination (SD), source-relay (SR), and relay-destination (RD) links, respectively. Therefore, an equivalent source-relay-destination (SRD) channel impulse response can be represented as $h_{SRD}[n] = h_{SR}[n] \star h_{RD}[n]$, where $\star$ denotes convolution operator and $L_{h_{SRD}} = L_{h_{SR}} + L_{h_{RD}} - 1$. Note that $L_{h_{SRD}}$, $L_{h_{SR}}$ and $L_{h_{RD}}$ refer to the length of $h_{SRD}[n]$, $h_{SR}[n]$ and $h_{RD}[n]$, respectively.

Michelle S. P. Facina and Moisés V. Ribeiro¸ Departament of Electrical Engineering, Federal University of Juiz de Fora, Juiz de Fora-MG, Brazil, E-mails: michelle.soares@engenharia.ufjf.br; mribeiro@ieee.org

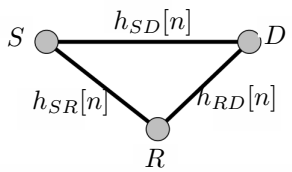

Fig. 1. Single relay cooperative model.

Let $T_C \geq 2T_S$, in which T_C and T_S denote the coherence time and the symbol period, respectively. Then, the vector representation of the channel impulse responses for SD, SR and RD links can be written as $\mathbf{h}_{SD} = [h_0 h_1 \dots h_{L_{SD}-1}]^T$, $\mathbf{h}_{SR} = [h_0 h_1 \dots h_{L_{SR}-1}]^T$, and $\mathbf{h}_{RD} = [h_0 h_1 \dots h_{L_{RD}-1}]^T$, respectively. Therefore, the vector representation of frequency responses of these channels are $\mathbf{H}_{SD} = \boldsymbol{\mathcal{F}}[\mathbf{h}_{SD}^T \, \mathbf{0}_{2N-L_{SD}}^T]^T$, $\mathbf{H}_{SR} = \boldsymbol{\mathcal{F}}[\mathbf{h}_{SR}^T \, \mathbf{0}_{2N-L_{SR}}^T]^T$, $\mathbf{H}_{RD} = \boldsymbol{\mathcal{F}}[\mathbf{h}_{RD}^T \, \mathbf{0}_{2N-L_{RD}}^T]^T$, in which $\boldsymbol{\mathcal{F}} = (1/\sqrt{2N})\mathbf{W}$, $\mathbf{W}$ is the $2N$-size discrete Fourier transform (DFT) matrix, and $\mathbf{0}_L$ is a L-length column vector constituted by zeros. Also, it is defined that $\boldsymbol{\mathcal{H}}_{SD} \triangleq \mathbf{diag}\{H_{SD}[0]\, H_{SD}[1] \dots H_{SD}[N-1]\}$, $\boldsymbol{\mathcal{H}}_{SR} \triangleq \mathbf{diag}\{H_{SR}[0]\, H_{SR}[1] \dots H_{SR}[N-1]\}$, and $\boldsymbol{\mathcal{H}}_{RD} \triangleq \mathbf{diag}\{H_{RD}[0]\, H_{RD}[1] \dots H_{RD}[N-1]\}$, in which $H_{SD}[k]$, $H_{SR}[k]$ and $H_{RD}[k]$ denote the kth coefficient of $\mathbf{H}_{SD}$, $\mathbf{H}_{SR}$, and $\mathbf{H}_{RD}$, respectively and **diag** represents the diagonal elements of a matrix. Also, it is defined that $\boldsymbol{\Lambda}_{|\boldsymbol{\mathcal{H}}_{SD}|^2} \triangleq \mathbf{diag}\{|H_{SD}[0]|^2\, |H_{SD}[1]|^2 \dots |H_{SD}[N-1]|^2\}$, $\boldsymbol{\Lambda}_{|\boldsymbol{\mathcal{H}}_{SR}|^2} \triangleq \mathbf{diag}\{|H_{SR}[0]|^2\, |H_{SR}[1]|^2 \dots |H_{SR}[N-1]|^2\}$, and $\boldsymbol{\Lambda}_{|\boldsymbol{\mathcal{H}}_{RD}|^2} \triangleq \mathbf{diag}\{|H_{RD}[0]|^2\, |H_{RD}[1]|^2 \dots |H_{RD}[N-1]|^2\}$ and $\boldsymbol{\mathcal{H}}_{SRD} = \boldsymbol{\mathcal{H}}_{SR}\boldsymbol{\mathcal{H}}_{RD}$.

The frequency domain representation of an OFDM symbol at the S node is $\mathbf{X} \in \mathbb{C}^{N\times 1}$, such that $\mathbb{E}\{\mathbf{X}\} = \mathbf{0}$, $\mathbb{E}\{\mathbf{X}\mathbf{X}^\dagger\} = \boldsymbol{\Lambda}_{\sigma_{\mathbf{X}}^2} = \sigma_{\mathbf{X}}^2\mathbf{I}_N$, where $\sigma_{\mathbf{X}}^2$ is the variance of $X[k]$ (the kth coefficient of the vector $\mathbf{X}$) and $\mathbf{I}_N$ is a N-size identity matrix, $\mathbb{E}\{.\}$ is the expectation operator and $\dagger$ is the conjugate transpose operator.

The frequency domain representation of N-length vectors for the additive noise for SD, SR, RD and SRD links are $\mathbf{V}_{SD}$, $\mathbf{V}_{SR}$, $\mathbf{V}_{RD}$ and $\mathbf{V}_{SRD} = \mathbf{V}_{RD} + \boldsymbol{\mathcal{H}}_{RD}\mathbf{V}_{SR}$. It is assumed that $\mathbb{E}\{\mathbf{V}_i \odot \mathbf{V}_j\} = \mathbb{E}\{\mathbf{V}_i\}\mathbb{E}\{\mathbf{V}_j\}$, $\forall i \neq j$, in which $\odot$ denotes the Hadamard product and $\mathbb{E}\{\mathbf{V}_i\} = \mathbf{0}$, $i,j \in \{SD, SR, RD\}$. Then $\mathbb{E}\{\mathbf{V}_i\mathbf{V}_i^\dagger\} = \boldsymbol{\Lambda}_{\boldsymbol{\sigma}^2_{\mathbf{V}_i}} = \mathbf{diag}\{\sigma^2_{\mathbf{V}_i}[0]\, \sigma^2_{\mathbf{V}_i}[1] \dots \sigma^2_{\mathbf{V}_i}[N-1]\}$ and $\mathbb{E}\{\mathbf{V}_{SRD}\mathbf{V}_{SRD}^\dagger\} = \boldsymbol{\Lambda}_{\boldsymbol{\sigma}^2_{\mathbf{V}_{SRD}}} = \boldsymbol{\Lambda}_{\boldsymbol{\sigma}^2_{\mathbf{V}_{RD}}} + \boldsymbol{\Lambda}_{\boldsymbol{\sigma}^2_{\mathbf{V}_{SR}}}\boldsymbol{\Lambda}_{|\boldsymbol{\mathcal{H}}_{RD}|^2}$.

Finally, for the DF protocol, in the first time slot, the source broadcasts data to the relay and destination and, then, the relay transmits data to the destination, in the second time slot. In this case, $L_{CP} = \max\{L_{SD}, L_{SR}\}$ in the first time slot and $L_{CP} = L_{RD}$ for the second time slot.

Assume that the total power is $P = P_0 + P_1$, where P_0 and P_1 are the powers allocated to the S node and R node to transmit data during the first and the second time slots, respectively. Each slot occupies the same time interval. In addition, the powers are optimally distributed among the subchannels ($\boldsymbol{\Lambda}_{P_0}$ and $\boldsymbol{\Lambda}_{P_1}$) for the subchannels of the symbol, that are transmitted by the S node in the first time slot and by the R node in the second time slot, respectively). Finally, perfect synchronization and channel state information at all nodes are assumed.

A. HS-OFDM with FDE-MMSE

For the FDE-MMSE, applied to the b link, the equalizer is $\boldsymbol{\mathcal{H}}_b^\dagger/(\boldsymbol{\mathcal{H}}_b^\dagger\boldsymbol{\mathcal{H}}_b + \frac{\boldsymbol{\Lambda}_{\sigma^2_{\mathbf{V}_b}}}{P_x\boldsymbol{\Lambda}_{\sigma^2_{\mathbf{X}}}})$, in which P_x is the power allocated to the subcarrier of the HS-OFDM symbol $\big(P_x \in \{\frac{P_0}{N}, \frac{P_1}{N}\}\big)$. For the SD link, the estimated symbol at the receiver is given by

$$\hat{\mathbf{X}}_{SD} = \frac{\sqrt{\frac{P_0}{N}}\boldsymbol{\Lambda}_{|\boldsymbol{\mathcal{H}}_{SD}|^2}\mathbf{X}}{\boldsymbol{\Lambda}_{|\boldsymbol{\mathcal{H}}_{SD}|^2} + \frac{\boldsymbol{\Lambda}_{\sigma^2_{\mathbf{V}_{SD}}}}{\frac{P_0}{N}\boldsymbol{\Lambda}_{\sigma^2_{\mathbf{X}}}}} + \frac{\boldsymbol{\mathcal{H}}_{SD}^\dagger\mathbf{V}_{SD}}{\boldsymbol{\Lambda}_{|\boldsymbol{\mathcal{H}}_{SD}|^2} + \frac{\boldsymbol{\Lambda}_{\sigma^2_{\mathbf{V}_{SD}}}}{\frac{P_0}{N}\boldsymbol{\Lambda}_{\sigma^2_{\mathbf{X}}}}}, \tag{1}$$

then, the signal-to-noise ratio (SNR) matrix is expressed by

$$\boldsymbol{\Lambda}_{\gamma_{SD}} = \frac{\sqrt{\frac{P_0}{N}}\boldsymbol{\Lambda}_{|\boldsymbol{\mathcal{H}}_{SD}|^2}}{\boldsymbol{\Lambda}_{\sigma^2_{\mathbf{V}_{SD}}}}\boldsymbol{\Lambda}_{\sigma^2_{\mathbf{X}}}. \tag{2}$$

By considering the SRD link, the use of the AF protocol provides a estimate of the transmitted symbol, which is expressed by

$$\hat{\mathbf{X}}_{AF,SRD} = \frac{\sqrt{\frac{P_0P_1}{N^2}}\boldsymbol{\Lambda}_{|\boldsymbol{\mathcal{H}}_{SRD}|^2}\mathbf{X}}{\boldsymbol{\Lambda}_{|\boldsymbol{\mathcal{H}}_{SRD}|^2} + \frac{\boldsymbol{\Lambda}_{\sigma^2_{\mathbf{V}_{SRD}}}}{\frac{P_0P_1}{N^2}\boldsymbol{\Lambda}_{\sigma^2_{\mathbf{X}}}}} + \frac{\sqrt{\frac{P_1}{N}}\boldsymbol{\mathcal{H}}_{SRD}^\dagger\boldsymbol{\mathcal{H}}_{RD}^\dagger\mathbf{V}_{SR}}{\boldsymbol{\Lambda}_{|\boldsymbol{\mathcal{H}}_{SRD}|^2} + \frac{\boldsymbol{\Lambda}_{\sigma^2_{\mathbf{V}_{SRD}}}}{\frac{P_0P_1}{N^2}\boldsymbol{\Lambda}_{\sigma^2_{\mathbf{X}}}}} + \frac{\boldsymbol{\mathcal{H}}_{SRD}^\dagger\mathbf{V}_{RD}}{\boldsymbol{\Lambda}_{|\boldsymbol{\mathcal{H}}_{SRD}|^2} + \frac{\boldsymbol{\Lambda}_{\sigma^2_{\mathbf{V}_{SRD}}}}{\frac{P_0P_1}{N^2}\boldsymbol{\Lambda}_{\sigma^2_{\mathbf{X}}}}} \tag{3}$$

and the SNR matrix is given by

$$\boldsymbol{\Lambda}_{\gamma_{AF,SRD}} = \frac{\frac{P_0P_1}{N^2}\boldsymbol{\Lambda}_{|\boldsymbol{\mathcal{H}}_{SRD}|^2}\boldsymbol{\Lambda}_{\sigma^2_{\mathbf{X}}}}{\frac{P_1}{N}\boldsymbol{\Lambda}_{|\boldsymbol{\mathcal{H}}_{RD}|^2}\boldsymbol{\Lambda}^2_{\sigma^2_{\mathbf{V}_{SR}}} + \boldsymbol{\Lambda}_{\sigma^2_{\mathbf{V}_{RD}}}}. \tag{4}$$

On the other hand, if the DF protocol is taken into account, then the estimated symbol at the receiver, through the SRD link, is given by

$$\mathbf{X}_{DF,SRD} = \frac{\sqrt{\frac{P_1}{N}}\boldsymbol{\Lambda}_{|\boldsymbol{\mathcal{H}}_{RD}|^2}}{\boldsymbol{\Lambda}_{|\boldsymbol{\mathcal{H}}_{RD}|^2} + \frac{\boldsymbol{\Lambda}_{\sigma^2_{\mathbf{V}_{RD}}}}{\frac{P_1}{N}\boldsymbol{\Lambda}_{\sigma^2_{\mathbf{X}}}}}\mathbf{X} + \frac{\sqrt{\frac{P_1}{N}}\boldsymbol{\Lambda}_{|\boldsymbol{\mathcal{H}}_{RD}|^2}}{\boldsymbol{\Lambda}_{|\boldsymbol{\mathcal{H}}_{RD}|^2} + \frac{\boldsymbol{\Lambda}_{\sigma^2_{\mathbf{V}_{RD}}}}{\frac{P_1}{N}\boldsymbol{\Lambda}_{\sigma^2_{\mathbf{X}}}}}\mathbf{E} + \frac{\boldsymbol{\mathcal{H}}_{RD}^\dagger}{\boldsymbol{\Lambda}_{|\boldsymbol{\mathcal{H}}_{RD}|^2} + \frac{\boldsymbol{\Lambda}_{\sigma^2_{\mathbf{V}_{RD}}}}{\frac{P_1}{N}\boldsymbol{\Lambda}_{\sigma^2_{\mathbf{X}}}}}\mathbf{V}_{RD} \tag{5}$$

and the SNR matrix is expressed by

$$\boldsymbol{\Lambda}_{\gamma_{DF,SRD}} = \frac{\frac{P_1}{N}\boldsymbol{\Lambda}_{|\boldsymbol{\mathcal{H}}_{RD}|^2}\boldsymbol{\Lambda}_{\sigma^2_{\mathbf{X}}}}{\frac{P_1}{N}\boldsymbol{\Lambda}_{|\boldsymbol{\mathcal{H}}_{RD}|^2}\boldsymbol{\Lambda}^2_{\sigma^2_{\mathbf{E}}} + \boldsymbol{\Lambda}_{\sigma^2_{\mathbf{V}_{RD}}}}, \tag{6}$$

where $\mathbf{E}$ denotes the error introduced by the symbol detection performed at the R node and $\boldsymbol{\Lambda}^2_{\sigma_{\mathbf{E}}}$=$E\{\mathbf{E}\mathbf{E}^\dagger\}$.

Considering the use of AF and DF protocols with MRC technique, the SNR matrices are given by (7) and (8), respectively.

Due to the fact that the in-home PLC channels are frequency selective and the additive noise is assumed to be a colored Gaussian random process, then, the maximum data rate can be evaluated, from (k,k) element of SNR matrix $\boldsymbol{\Lambda}_\gamma$, by using

$$\mathbf{\Lambda}_{\gamma_{AF,MRC}} = \frac{\left(\frac{\sqrt{\frac{P_0}{N}}\mathbf{\Lambda}_{SD}\mathbf{\Lambda}_{|\boldsymbol{\mathcal{H}}_{SD}|^2}}{\mathbf{\Lambda}_{|\boldsymbol{\mathcal{H}}_{SD}|^2+\frac{\mathbf{\Lambda}_{\sigma^2_{\mathbf{V}_{SD}}}}{\frac{P_0}{N}\mathbf{\Lambda}_{\sigma^2_{\mathbf{X}}}}}} + \frac{\sqrt{\frac{P_0P_1}{N^2}}\mathbf{\Lambda}_{AF,SRD}\mathbf{\Lambda}_{|\boldsymbol{\mathcal{H}}_{SRD}|^2}}{\mathbf{\Lambda}_{|\boldsymbol{\mathcal{H}}_{SRD}|^2+\frac{\mathbf{\Lambda}_{\sigma^2_{\mathbf{V}_{SRD}}}}{\frac{P_0P_1}{N^2}\mathbf{\Lambda}_{\sigma^2_{\mathbf{X}}}}}} \right)^2 \mathbf{\Lambda}_{\sigma^2_{\mathbf{X}}}}{\frac{\mathbf{\Lambda}^2_{SD}\mathbf{\Lambda}_{|\boldsymbol{\mathcal{H}}_{SD}|^2}}{\left(\mathbf{\Lambda}_{|\boldsymbol{\mathcal{H}}_{SD}|^2+\frac{\mathbf{\Lambda}_{\sigma^2_{\mathbf{V}_{SD}}}}{\frac{P_0}{N}\mathbf{\Lambda}_{\sigma^2_{\mathbf{X}}}}}\right)^2}\mathbf{\Lambda}_{\sigma^2_{\mathbf{V}_{SD}}} + \frac{\mathbf{\Lambda}^2_{AF,SRD}\mathbf{\Lambda}_{|\boldsymbol{\mathcal{H}}_{SRD}|^2}\mathbf{\Lambda}_{\sigma^2_{\mathbf{V}_{RD}}}}{\left(\mathbf{\Lambda}_{|\boldsymbol{\mathcal{H}}_{SRD}|^2+\frac{\mathbf{\Lambda}_{\sigma^2_{\mathbf{V}_{SRD}}}}{\frac{P_0P_1}{N^2}\mathbf{\Lambda}_{\sigma^2_{\mathbf{X}}}}}\right)^2} + \frac{\frac{P_1}{N}\mathbf{\Lambda}^2_{AF,SRD}\mathbf{\Lambda}_{|\boldsymbol{\mathcal{H}}_{SRD}|^2}\mathbf{\Lambda}_{|\boldsymbol{\mathcal{H}}_{RD}|^2}}{\left(\mathbf{\Lambda}_{|\boldsymbol{\mathcal{H}}_{SRD}|^2+\frac{\mathbf{\Lambda}_{\sigma^2_{\mathbf{V}_{SRD}}}}{\frac{P_0P_1}{N^2}\mathbf{\Lambda}_{\sigma^2_{\mathbf{X}}}}}\right)^2}\mathbf{\Lambda}_{\sigma^2_{\mathbf{V}_{SR}}}}, \tag{7}$$

where $\mathbf{\Lambda}_{SD} = \frac{\mathbf{\Lambda}_{\gamma_{SD}}}{\mathbf{\Lambda}_{\gamma_{SD}}+\mathbf{\Lambda}_{\gamma_{AF,SRD}}}$ and $\mathbf{\Lambda}_{AF,SRD} = \frac{\mathbf{\Lambda}_{\gamma_{AF,SRD}}}{\mathbf{\Lambda}_{\gamma_{SD}}+\mathbf{\Lambda}_{\gamma_{AF,SRD}}}$.

$$\mathbf{\Lambda}_{\gamma_{DF,MRC}} = \frac{\left(\frac{\sqrt{\frac{P_0}{N}}\mathbf{\Lambda}_{SD}\mathbf{\Lambda}_{|\boldsymbol{\mathcal{H}}_{SD}|^2}}{\mathbf{\Lambda}_{|\boldsymbol{\mathcal{H}}_{SD}|^2+\frac{\mathbf{\Lambda}_{\sigma^2_{\mathbf{V}_{SD}}}}{\frac{P_0}{N}\mathbf{\Lambda}_{\sigma^2_{\mathbf{X}}}}}} + \frac{\sqrt{\frac{P_1}{N}}\mathbf{\Lambda}_{DF,SRD}\mathbf{\Lambda}_{|\boldsymbol{\mathcal{H}}_{RD}|^2}}{\mathbf{\Lambda}_{|\boldsymbol{\mathcal{H}}_{RD}|^2+\frac{\mathbf{\Lambda}_{\sigma^2_{\mathbf{V}_{RD}}}}{\frac{P_1}{N}\mathbf{\Lambda}_{\sigma^2_{\mathbf{X}}}}}} \right)^2 \mathbf{\Lambda}_{\sigma^2_{\mathbf{X}}}}{\frac{\mathbf{\Lambda}^2_{SD}\mathbf{\Lambda}_{|\boldsymbol{\mathcal{H}}_{SD}|^2}}{\left(\mathbf{\Lambda}_{|\boldsymbol{\mathcal{H}}_{SD}|^2+\frac{\mathbf{\Lambda}_{\sigma^2_{\mathbf{V}_{SD}}}}{\frac{P_0}{N}\mathbf{\Lambda}_{\sigma^2_{\mathbf{X}}}}}\right)^2}\mathbf{\Lambda}_{\sigma^2_{\mathbf{V}_{SD}}} + \mathbf{\Lambda}^2_{DF,SRD}\left[\frac{\frac{P_1}{N}\mathbf{\Lambda}_{|\boldsymbol{\mathcal{H}}_{RD}|^4}}{\left(\mathbf{\Lambda}_{|\boldsymbol{\mathcal{H}}_{RD}|^2+\frac{\mathbf{\Lambda}_{\sigma^2_{\mathbf{V}_{RD}}}}{\frac{P_1}{N}\mathbf{\Lambda}_{\sigma^2_{\mathbf{X}}}}}\right)^2}\mathbf{\Lambda}_{\sigma^2_{\mathbf{E}}} + \frac{\mathbf{\Lambda}_{|\boldsymbol{\mathcal{H}}_{RD}|^2}}{\left(\mathbf{\Lambda}_{|\boldsymbol{\mathcal{H}}_{RD}|^2+\frac{\mathbf{\Lambda}_{\sigma^2_{\mathbf{V}_{RD}}}}{\frac{P_1}{N}\mathbf{\Lambda}_{\sigma^2_{\mathbf{X}}}}}\right)^2}\mathbf{\Lambda}_{\sigma^2_{\mathbf{V}_{RD}}}\right]}, \tag{8}$$

where $\mathbf{\Lambda}_{SD} = \frac{\mathbf{\Lambda}_{\gamma_{SD}}}{\mathbf{\Lambda}_{\gamma_{SD}}+\mathbf{\Lambda}_{\gamma_{DF,SRD}}}$ and $\mathbf{\Lambda}_{DF,SRD} = \frac{\mathbf{\Lambda}_{\gamma_{DF,SRD}}}{\mathbf{\Lambda}_{\gamma_{SD}}+\mathbf{\Lambda}_{\gamma_{DF,SRD}}}$.

$$R = \max_{\mathbf{\Lambda}_{P_0},\mathbf{\Lambda}_{P_1}} \frac{B_w}{2N+L_{CP}} \sum_{k=0}^{N-1} \log_2[1+\mathbf{\Lambda}_{\gamma}(k,k)] \ , \tag{9}$$

subject to $\mathrm{Tr}(\mathbf{\Lambda}_{P_0}) = P_0$, $\mathrm{Tr}(\mathbf{\Lambda}_{P_1}) = P_1$, B_w is the frequency bandwidth and Tr is the trace operator. $\mathbf{\Lambda}_{P_0} = \mathbf{diag}\left\{P_{0,0}P_{0,1} \ \ldots \ P_{0,N-1}\right\}$ and $\mathbf{\Lambda}_{P_1} = \mathbf{diag}\left\{P_{1,0}P_{1,1} \ \ldots \ P_{1,N-1}\right\}$, for the SD, SR and SRD links with the AF protocol and SRD link with the DF protocol, respectively.

III. Measurement Campaign

To analyze the effects of the symbol detection error on the use of the DF protocol at the R node, a measurement campaign to acquire estimates of cooperative and in-home PLC channels was carried out in Juiz de Fora, Brazil.

For the characterization of such PLC channels, seven middle class residences in a typical urban area were considered. The used measurement setup is composed of two rugged personal computers equipped with data acquisition and generation boards connected to the power cable by a coupling circuit [5]. The coupler is constituted by a high pass filter that blocks the main voltages (50 or 60 Hz) in order to avoid equipment damage. With this equipment, it is constructed the setup of Fig. 2. Firstly, the signal is generated in the waveform generation board (Tx) and injected into the power cable through the electrical outlet. On the other side of the electric power grids, the extracted signal is digitized by a data acquisition board (Rx).

Also, a sounding-based method was applied to estimate the frequency response of the measured channels [4]. The set of parameters used in the methodology to estimate the frequency response of in-home PLC channels is summarized in Table I.

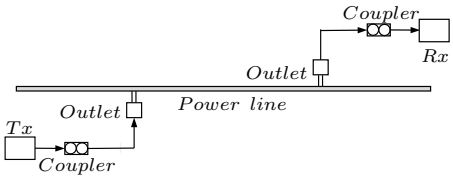

Fig. 2. An example of the use of the measurement setup.

In this measurement campaign, more than $36,000$ estimates of in-home PLC channels, whose physical electric circuits cover distances from 2 to 10 m, were obtained from the measured data and classified as SD, SR or RD links. The frequency band from 1.7 MHz up 100 MHz was considered.

TABLE I
Main parameters adopted by the technique applied to estimate the PLC channel frequency responses.

Description	Value
Sampling frequency	$f_s = 200$ MHz
Number of sub-carriers	$N = 2048$
Modulation	BPSK
Cyclic prefix length	$L_{cp} = 512$
Frequency resolution	48.83 kHz
Symbol duration	23.04 μs

Fig. 3 shows the adopted locations for the R node during the measurement campaign. Basically, the R node was located in the middle between the S and D nodes (case #1); near the D node (case #2); near the S node (case #3); and far from both S and D nodes (case #4). In these cases the relay, the source and the destination nodes belong to the same electrical circuit. The analysis of these cases can reveal in which locations the R node can benefit in-home PLC systems.

Fig. 4 shows the mean values of amplitude spectra of

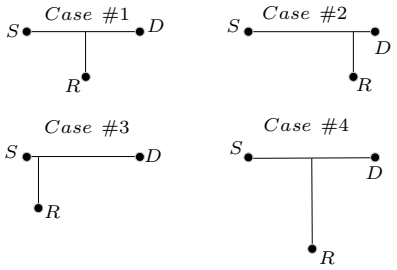

Fig. 3. Relay locations based on electrical wiring distances.

measured PLC channel frequency responses for SD, SR, RD, and SRD links for case #1, case #2, case #3 and case #4, respectively. Regarding case #1 (Fig. 4a), it can be seen that the attenuation profiles for SR and RD links are lower than that noted in the SD link (distances involving the SD link are longer), which is in accordance with the theory related to the wave propagation in a non-ideal conductor (attenuation increases with frequency and distance). A carefully analysis of this plot indicates that the use of the DF protocol at the R node may result in improved performance if the errored symbol detection probability at the R node tends to zero. On the other hand, the attenuation profiles of channel frequency responses for the SRD link show that attenuation is extremely high and, as a consequence, the AF protocol may not offer improvement.

Following the same reasoning, in Fig. 4b, we can note that the RD link shows the lowest attenuation, as expected, since the R node is closest to the destination. On the other hand, in case #3, as the R node is near the source, then the SR link shows the lowest attenuation, see Fig. 4c. Finally, in Fig. 4d, there is a strong attenuation for SR, RD and SRD links. Thus, when the R node is away from the S and the D nodes, cooperation may not be advantageous.

Finally, Fig. 5 depicts estimates of the power spectral density (PSD) of the measured additive noise for the SD, SR, and RD links for case #1. For simplicity, the curves of the other cases are not showed. But it is noteworthy that they exhibit similar behavior to the case #1. The reason for this is the fact that the electric circuit works as a bus, therefore, a significant change of the PSD of the noise, in the same electric circuit, is not expected. Due to the fact that the PSDs of SD and RD links refer to the additive noise at the D node measured during slots #1 and #2, it is assumed the mean value of the PSD of both SD and RD links in the simulation results.

IV. Results

This section presents the maximum data rate analyses of the measured cooperative and in-home and cooperative PLC channels based on averages of estimates of channel frequency responses and PSD for HS-OFDM scheme. In order to evaluate the cooperative and in-home PLC system performance when $\mathbf{E} \neq \mathbf{0}$, it is presented the maximum data rates for all cases when HS-OFDM scheme, frequency domain equalizer (FDE) with minimum mean square error (MMSE), MRC technique, $P = 20$ dBm, $N = 4096$, $B_w = 100$ MHz are considered and the transmission power is optimally allocated by using

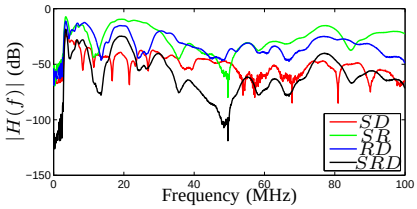

(a) case #1: midway.

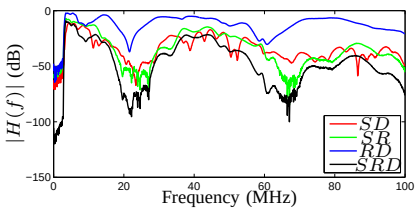

(b) case #2: near D node.

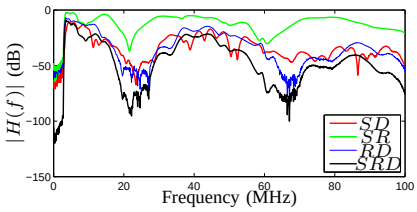

(c) case #3: near S node.

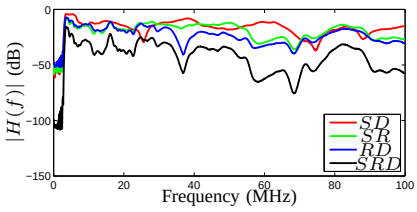

(d) case #4: far from S and D nodes.

Fig. 4. Attenuation profiles of the frequency response of SD, SR, RD, and SRD links.

the water filling technique. Also, it is assumed that $\mathbf{E}$ is modeled as circular complex Gaussian such that $\mathbb{E}\{\mathbf{E}\} = \mathbf{0}$ and $\mathbb{E}\{\mathbf{E}\mathbf{E}^{\dagger}\} = \mathbf{\Lambda}_{\sigma^2_{\mathbf{E}}}$.

In order to verify the influence symbol detection error on cooperative in-home PLC based on HS-OFDM scheme, the maximum data rate was evaluated when $P \in \{-20, -10, 0, 10, 20, 30\}$ dBm and the choice of P_0 and P_1 and their distribution among the subcarriers are those that maximize the mutual information between the transmitted and received signals. Fig. 6 shows the normalized maximum data rate for the AF and DF protocols for each case when

$$\bar{C}_{\beta} = \frac{C_{\beta}}{C_{\max}}, \tag{10}$$

in which $\beta \in \{\text{AF,DF}\}$ and $C_{\max} = \max_{P_0} C_{SD}$ subject to $P_0 + P_1 \leq P$ is the achievable data rate associated with the SD link. The value of k was varied according to the ratio $k = 10 \times \log_{10}\left[\frac{\mathrm{Tr}\left(\mathbf{\Lambda}_{P_1}\mathbf{\Lambda}_{|\boldsymbol{\mathcal{H}}_{RD}|^2}\mathbf{\Lambda}_{\sigma^2_{\mathbf{E}}}\right)}{\mathrm{Tr}\left(\mathbf{\Lambda}_{\sigma^2_{\mathbf{V}_{RD}}}\right)}\right]$, formed from the relationship between the terms related to the error symbol

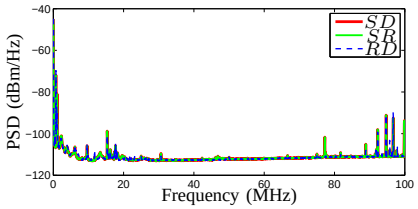

Fig. 5. PSD of measured additive noises in the SD, SR, and RD links.

detection and noise of RD link. The obtained results are shown in Fig. 6. It can be observed that, as k increases, the maximum data rate related to the DF protocol decreases. In Fig. 6a, it can be noted that the DF protocol is not advantageous for $k \geq 40$ dB and $k \geq 30$ dB when FDE-MMSE and FDE-ZF are, respectively, considered for case #1. On the other hand, Fig. 6b shows that for $k > 60$ dB (FDE-MMSE) and $k \geq 48$ dB (FDE-ZF), the DF protocol is not better than the AF one for case #2. Already for case #3 (Fig. 6c, when $k > 60$ dB (FDE-MMSE) and $k \geq 38$ dB (FDE-ZF) there is not advantage in using the DF protocol. Finally, for case #4 (Fig. 6d, both protocols show similar performances. To better represent the plots of Figures, the maximum data rate was normalized by the following factors: 5 Mbps (case #1), 8.75 Mbps (cases #2 and #3) and 5.6 Mbps (case #4). Furthermore, it can observed that the FDE-MMSE is more robust than the FDE-ZF when the error symbol detection at the relay node increases.

V. Conclusions

This paper has presented analyses based on the data obtained from a measurement campaign of cooperative and in-home PLC channels and additive noises by considering a single relay model and the frequency band 1.7-100 MHz.

Based on the provided analyses, we presented maximum data rate of a HS-OFDM scheme regarding AF and the DF protocols together with MRC technique. We observed that FDE-MMSE is more robust than FDE-ZF when the symbol detection error increases at the relay. Additionally, the DF protocol presents gains in scenarios where the relay node is approximately at the midpoint between the S and D nodes and also when it is near to the S or D node. Finally, we showed that when the DF protocol is adopted at the relay node, it stops being advantageous in relation to the AF protocol as the symbol error probability at the relay node increases considerably. This result is according to the previous analysis made from the frequency responses in Section III.

Acknowledgment

The authors would like to thank CNPq, CAPES, FAPEMIG, FINEP, P&D ANEEL-CEMIG, INERGE and Smarti9 Ltda. for their support of this research.

References

[1] G. Bumiller, L. Lampe, and H. Hrasnica, "Power line communication networks for large-scale control and automation systems," *IEEE Communications Magazine*, vol. 48, no. 4, pp. 106–113, Apr. 2010.

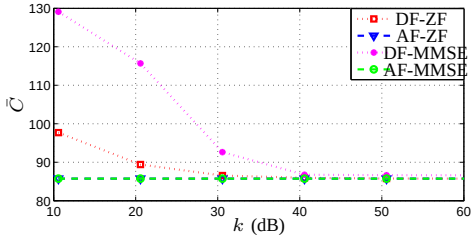

(a) case #1

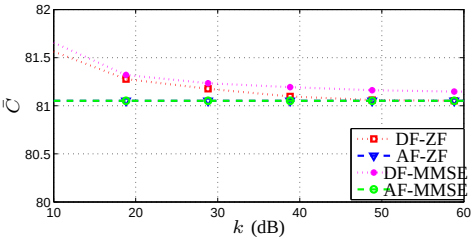

(b) case #2

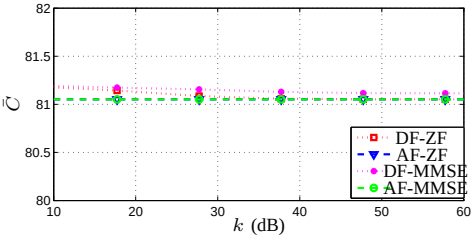

(c) case #3

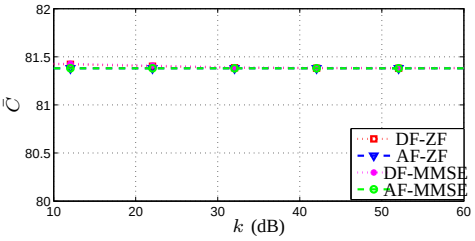

(d) case #4

Fig. 6. Maximum data rates when $\mathbf{E} \neq \mathbf{0}$, $P = 20$ dBm and HS-OFDM are considered.

[2] S. D'Alessandro, A. Tonello, and F. Versolatto, "Power savings with opportunistic decode and forward over in-home plc networks," in *IEEE International Symposium on Power Line Communications and Its Applications*, Apr. 2011, pp. 176–181.

[3] M. S. P. Facina and M. V. Ribeiro, "The influence of transmission power and frequency bandwidth on in-home cooperative power line communication," in *Proc. IEEE International Symposium on Power Line Communications and its Applications*, Mar. 2015.

[4] A. A. M. Picorone, Oliveira, T. R., and M. V. Ribeiro, "PLC channel estimation based on pilots signal for OFDM modulation: A review," *IEEE Latin America Transactions*, vol. 12, no. 4, pp. 580–589, Jun. 2014.

[5] G. Colen, C. Marques, T. Oliveira, F. de Campos, and M. Ribeiro, "Measurement setup for characterizing low-voltage and outdoor electric distribution grids for PLC systems," in *IEEE PES Conference On Innovative Smart Grid Technologies Latin America*, Apr. 2013, pp. 1–5.